Effect of gasification agent on the performance of solid oxide fuel cell and biomass gasification systems

Colpan, C. Ozgur; Hamdullahpur, Feridun; Dincer, Ibrahim; Yoo, Yeong

Publisher's version / Version de l'éditeur:
https://doi.org/10.1016/j.ijhydene.2009.08.083
International Journal of Hydrogen Energy, 35, 10, pp. 5001-5009, 2009

Available at www.sciencedirect.com

ScienceDirect

journal homepage: www.elsevier.com/locate/he

Effect of gasification agent on the performance of solid oxide fuel cell and biomass gasification systems

C. Ozgur Colpan [a,*], Feridun Hamdullahpur [b], Ibrahim Dincer [c], Yeong Yoo [d]

[a] Mechanical and Aerospace Engineering Department, Carleton University, 1125 Colonel By Drive, Ottawa, Ontario, Canada K1S 5B6
[b] Mechanical and Mechatronics Engineering Department, University of Waterloo, 200 University Avenue West, Waterloo, Ontario, Canada N2L 3G1
[c] Faculty of Engineering and Applied Science, University of Ontario Institute of Technology, 2000 Simcoe Street North, Oshawa, Ontario, Canada L1H 7L7
[d] National Research Council of Canada, Institute for Chemical Process and Environmental Technology, Ottawa, Ontario, Canada K1A 0R6

ARTICLE INFO

Article history:
Received 18 June 2009
Received in revised form
11 August 2009
Accepted 30 August 2009
Available online 3 October 2009

Keywords:
Solid oxide fuel cell
Biomass
Gasification
Energy
Exergy
Efficiency

ABSTRACT

In this paper, an integrated solid oxide fuel cell (SOFC) and biomass gasification system is modeled to study the effect of gasification agent (air, enriched oxygen and steam) on its performance. In the present modeling, a heat transfer model for SOFC and thermodynamic models for the rest of the components are used. In addition, exergy balances are written for the system components. The results show that using steam as the gasification agent yields the highest electrical efficiency (41.8%), power-to-heat ratio (4.649), and exergetic efficiency (39.1%), but the lowest fuel utilization efficiency (50.8%). In addition, the exergy destruction is found to be the highest at the gasifier for the air and enriched oxygen gasification cases and the heat exchanger that supplies heat to the air entering the SOFC for the steam gasification case.

1. Introduction

Biomass has increased its importance due to the fact that it can be utilized as a potential fuel source in advanced energy systems. In addition, systems based on biomass fuel are considered to contribute to the sustainable development in industrialized and developing countries. In this regard, researchers tend to find solutions to obtain efficient and economical heat and electricity generation from biomass fuel.

There are various types of biomass, such as wood, landfill gas, crops, alcohol fuels, and municipal solid wastes. Biomass has a share of 10.7% in the total global primary energy use and 1.1% in the world electricity production [1]. It is expected that the biomass share of electricity output will increase to a point between 2% and 5.1% in 2050 according to the different scenarios [2]. Conventionally, biomass is converted to electricity by combustion of the feedstock to generate steam that is used to drive the steam turbine. Other technologies include externally fired gas turbines, integrated gasification combined cycles, and fuel cells.

Among the different types of fuel cells, molten carbonate fuel cell (MCFC) and SOFC are considered as the most promising ones for biomass fuelled fuel cells due to their high operating temperature level, flexibility to different fuel, and

* Corresponding author.
E-mail address: cocolpan@connect.carleton.ca (C.O. Colpan).
0360-3199/$ – see front matter © 2009 Professor T. Nejat Veziroglu. Published by Elsevier Ltd. All rights reserved.
doi:10.1016/j.ijhydene.2009.08.083

greater tolerance to contaminants. According to the biomass conversion method, some of the other fuel cell types may also be useful. For example, landfill gas and digester gas may be used with phosphoric acid fuel cell (PAFC) today and their usage with this kind of fuel cell has been successfully demonstrated [3]. In addition, the suitability of biogas as a fuel for proton exchange membrane fuel cell (PEMFC) has been experimentally confirmed [4].

Biomass fuelled integrated SOFC system is one of the key energy technologies of the future since it combines the merits of renewable energy sources and hydrogen energy systems. There has been an increasing interest in converting biomass to a product gas by various thermochemical and biochemical methods for using it as a fuel in SOFCs. These methods include gasification, anaerobic digestion, fast pyrolysis, and fermentation. The product gas obtained from these conversions contains contaminants such as tars, hydrogen sulfide, and alkali compounds, which should be cleaned up according to the tolerance level of the SOFC to these contaminants. The cleaned gas exiting the gas cleanup system should be reformed to hydrogen and carbon monoxide to be utilized in the SOFC, which might be inside or outside the stack.

Panopoulos et al. [5,6] investigated the integration of a SOFC with a novel allothermal biomass steam gasification process. They calculated the electrical efficiency of the system as 36% and exergetic efficiency as 32%. Cordiner et al. [7] studied the integration of a downdraft gasifier with a SOFC in which woody material is used as the fuel. Electrical efficiency of the system was calculated as 45.8%. In the paper by Athanasiou et al. [8], integrated SOFC, steam turbine, and gasifier system was studied in terms of thermodynamics. The electrical efficiency of the system was found to be 43.3%. The comparison of cold gas cleanup and hot gas cleanup systems to be used in biomass gasification and SOFC system was done by Omosun et al. [9]. After taking into account thermodynamic and economical considerations, they concluded that hot gas cleanup should be preferred.

The main objective of this study is to develop a thermal model for an integrated SOFC and biomass gasification system and investigate the effect of gasification agent on the performance of this system. For this purpose, thermodynamic models are developed for the system components, except SOFC, e.g. gasifier, afterburner, and blower. For the SOFC, a heat transfer model (see details in [10]) is employed. Some performance assessment parameters, namely: electrical efficiency, fuel utilization efficiency, power-to-heat ratio, and exergetic efficiency are studied. Also, exergy balances are written for the system components to calculate the exergy destructions within the system and exergy losses to the environment.

2. Description of the system

A schematic of the integrated biomass gasification and SOFC system is shown in Fig. 1. In this system, biomass enters the dryer to bring its moisture content to a level acceptable by the gasifier. According to the gasification agent, one of the following substances enters the gasifier: air, enriched oxygen or steam. The gas produced by gasification, which is called syngas, has high amounts of tar, sulphur and other contaminants which may cause degradation in SOFCs. Due to this fact, a gas cleanup should be used to clean the syngas according to the SOFC impurity levels. In this study, a hot gas cleanup is chosen. The cleaned syngas enters the SOFC, where electricity is produced. To prevent the carbon deposition, anode recirculation ratio is adjusted. The depleted fuel and air streams enter the afterburner to burn the unused fuel and increase the temperature of these streams. The burned gas mixture enters the heat exchanger to supply heat to the air entering the SOFC. The gas mixture leaving the heat exchanger supplies heat to the following devices: the steam generator and the gasifier in the case of steam gasification and the dryer. It is then emitted to the atmosphere.

A number is given to each state. In Fig. 1, states 20 and 22 are valid for both the air and enriched oxygen gasification cases. State 21 is only valid for enriched oxygen gasification case. State 13a, 13b, and 19 are only valid for the steam

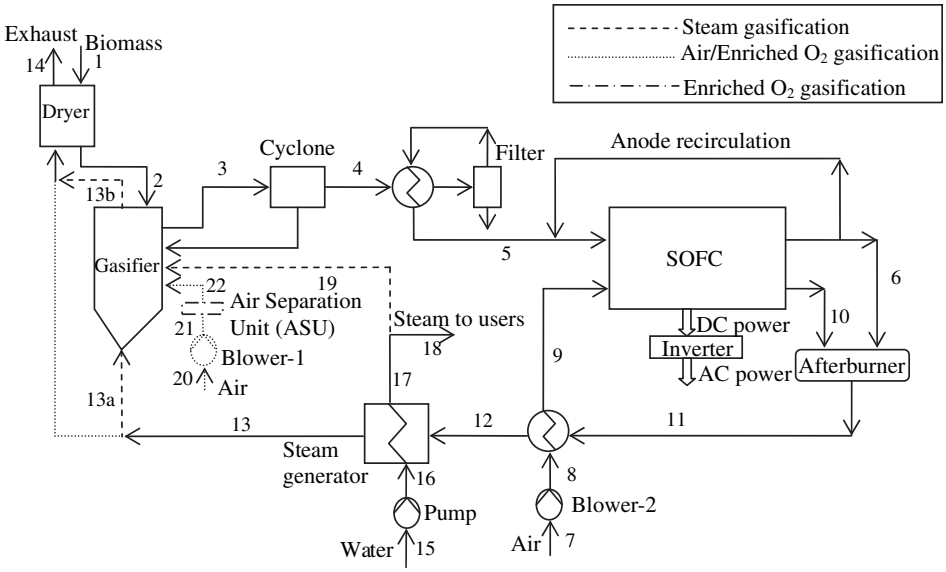

Fig. 1 – Schematic of the integrated biomass gasification and SOFC system.

gasification case. The differences in the configurations are represented with different dashed lines, which are labelled on Fig. 1.

3. Modeling

The main approach in the modeling is as follows. The syngas composition is first calculated using the gasifier model. Then, this composition and other SOFC operating parameters are used as input parameters in the heat transfer model of the SOFC. This model gives us the molar flow rate at the inlet and exit of gas channels, power output, and temperature at the exit of gas channels for a single cell. According to the power requirement of the SOFC, the number of SOFC stacks that must be used in this system is found. Then, using the output data from the gasifier and SOFC models, the molar flow rate of dry biomass is calculated. Using this molar flow rate and applying energy balances to the remaining components, the enthalpy flow rate of all states, work input to the blowers and pump, if applicable, are calculated.

The main assumptions in this model are as follows:

- The system operates at steady state.
- Kinetic and potential energy effects are ignored.
- Ideal gas principles apply for the gases.
- The syngas produced by the gasifier is at chemical equilibrium.
- The impurities such as tar, sulphur, ammonia are not considered in the calculations.
- Heat losses from the components are neglected.
- Work input for the high temperature blower for anode recirculation is neglected.
- All of the steam export returns as condensate.
- Complete combustion occurs in the combustor.

As an example, the modeling equations for the steam gasification case are given below.

The chemical reaction in the dryer may be shown as:

$$C_xH_yO_z + m_1H_2O_{(l)} \rightarrow C_xH_yO_z + m_2H_2O_{(l)} + (m_1 - m_2)H_2O_{(v)} \quad (1)$$

The gasification reaction may be given as:

$$C_xH_yO_z + m_2H_2O_{(l)} + (m_1 - m_2)H_2O_{(v)} + \lambda H_2O_{(v)} + q_{added} \rightarrow \alpha_1CH_4 + \alpha_2H_2 + \alpha_3CO + \alpha_4CO_2 + \alpha_5H_2O \quad (2)$$

In Eq. (2), if we fix λ, there are six unknowns: α_1,α_2, α_3, α_4, α_5, and q_{added}. We need six equations to find these unknowns. These equations are 3 atom balances, Eqs. (3)–(5), chemical equilibrium relations for water–gas shift reaction and methanation reaction, Eqs. (6) and (7), and the energy balance around the control volume enclosing the gasifier, Eq. (8).

$$x = \alpha_1 + \alpha_3 + \alpha_4 \quad (3)$$

$$y + 2m_1 + 2\lambda = 4\alpha_1 + 2\alpha_2 + 2\alpha_5 \quad (4)$$

$$z + m_1 + \lambda = \alpha_3 + 2\alpha_4 + \alpha_5 \quad (5)$$

$$K_{wgs} = \exp\left[-\Delta\overline{g}^{\circ}_{wgs}/RT\right] = \frac{x_{CO_2}\cdot x_{H_2}}{x_{CO}\cdot x_{H_2O}} \quad (6)$$

$$K_m = \exp\left[-\Delta\overline{g}^{\circ}_{wgs}/RT\right] = \frac{x_{CH_4}}{x_{H_2}^2}\cdot\left(\frac{P}{P_o}\right)^{-1} \quad (7)$$

$$\overline{h}^{\circ}_{2,C_xH_yO_z} + m_2\cdot\overline{h}^{\circ}_{2,H_2O(l)} + (m_1 - m_2)\cdot\overline{h}^{\circ}_{2,H_2O(v)} + \lambda\cdot\overline{h}^{\circ}_{19,H_2O(v)} + q_{added} = \alpha_1\overline{h}^{\circ}_{3,CH_4} + \alpha_2\overline{h}^{\circ}_{3,H_2} + \alpha_3\overline{h}^{\circ}_{3,CO} + \alpha_4\overline{h}^{\circ}_{3,CO_2} + \alpha_5\overline{h}^{\circ}_{3,H_2O} \quad (8)$$

In a previous paper of the authors [11], a thermodynamic model of a direct internal reforming SOFC, which was based on 0-D modeling technique, was presented. In this paper, a better model for SOFC that includes the heat transfer mechanisms is used. Details on the model equations for the SOFC are available elsewhere [10]. The modeling technique and the main features of the heat transfer model of the SOFC used in this study are as follows:

- A control volume around the repeat element of a planar, co-flow, and direct internal reforming SOFC is taken.
- Solid structure is modeled in 2-D, whereas gas channels are modeled in 1-D.
- Cell voltage, Reynolds number at the fuel channel inlet, and excess air coefficient are the main input parameters. Current density, temperature and molar gas composition distributions, fuel utilization, power output, and electrical efficiency of the cell are the main output parameters.
- Six gas species (CH_4, H_2, CO, CO_2, H_2O and N_2) at the fuel channel inlet and two gas species (O_2 and N_2) at the air channel inlet are considered.
- Fully developed laminar flow conditions are assumed in the air and fuel channels.
- Convection in the rectangular ducts, surface-to-surface radiation effects, conduction heat transfer at the section where the interconnects are in contact with Positive-Electrolyte-Negative (PEN) structure, and ohmic, activation and concentration polarizations are considered.
- The code is written in MatLAB.
- The model is validated with the results from IEA Benchmark Test [12].

Using the SOFC model discussed above, the code developed for the heat transfer model is run several times to obtain a desired fuel utilization for a given cell geometry, cell voltage, Reynolds number and excess air coefficient. Using this code, output for a single cell is obtained. For this output, number of stacks needed for the system can be calculated as follows:

$$n_{stack} = \frac{\dot{W}_{req,SOFC}}{w_{SOFC}\cdot n_{cps}} \quad (9)$$

We should take the closest integer higher than the value obtained by Eq. (9). Then, power output of SOFC and molar flow rate of gas species at the inlets and exits of fuel and air channels can be calculated for the total amount of stacks calculated.

At this point, we can calculate the molar flow rate of dry biomass entering the system using Eq. (10).

$$\dot{n}_{C_xH_yO_z} = \frac{\sum_{k=1}^{5} \dot{n}_{k,fc.inlet}}{\alpha_1 + \alpha_2 + \alpha_3 + \alpha_4 + \alpha_5} \quad (10)$$

If we consider complete combustion in the afterburner, the chemical reaction occurring in the afterburner may be given as

$$\dot{n}_{6,CH_4}CH_4 + \dot{n}_{6,H_2}H_2 + \dot{n}_{6,CO}CO + \dot{n}_{6,CO_2}CO_2 + \dot{n}_{6,H_2O}H_2O + \dot{n}_{6,N_2}N_2 + \dot{n}_{10,O_2}O_2 + \dot{n}_{10,N_2}N_2 \rightarrow \dot{n}_{11,CO_2}CO_2 + \dot{n}_{11,H_2O}H_2O + \dot{n}_{11,O_2}O_2 + \dot{n}_{11,N_2}N_2 \quad (11)$$

The molar flow rates of gas species at states 6 and 10 are known from the SOFC model. We can calculate the molar flow rates of gas species at state 11 using the atom balances, as given in Eqs. (12)–(15); and the enthalpy flow rate of this state can be found using an energy balance around the control volume enclosing the afterburner, as given in Eq. (16).

$$\dot{n}_{11,CO_2} = \dot{n}_{6,CH_4} + \dot{n}_{6,CO} + \dot{n}_{6,CO_2} \quad (12)$$

$$\dot{n}_{11,H_2O} = 2\cdot\dot{n}_{6,CH_4} + \dot{n}_{6,H_2} + \dot{n}_{6,H_2O} \quad (13)$$

$$\dot{n}_{11,O_2} = \dot{n}_{6,CO}/2 + \dot{n}_{6,CO_2} + \dot{n}_{6,H_2O}/2 + \dot{n}_{10,O_2} - \dot{n}_{11,CO_2} - \dot{n}_{11,H_2O}/2 \quad (14)$$

$$\dot{n}_{11,N_2} = \dot{n}_{6,N_2} + \dot{n}_{10,N_2} \quad (15)$$

$$\dot{H}_{11} = \sum_{k=1}^{6}\left(\dot{n}_{6,k}\cdot\overline{h}_{6,k}\right) + \sum_{l=1}^{2}\left(\dot{n}_{10,l}\cdot\overline{h}_{10,l}\right) \quad (16)$$

where k denotes CH_4, H_2, CO, CO_2, H_2O and N_2; whereas l denotes O_2 and N_2.

The specific enthalpy of state 8 may be written as:

$$\overline{h}_8 = \overline{h}_7 + \frac{(P_8 - P_7)\cdot M_{air}}{\rho_{air}\cdot\eta_{blower}} \quad (17)$$

Specific work input to blower may be given as

$$\dot{W}_{blower} = \left(\dot{n}_{9,O_2} + \dot{n}_{9,N_2}\right)\cdot\left(\overline{h}_8 - \overline{h}_7\right) \quad (18)$$

From an energy balance around the control volume enclosing the heat exchanger, enthalpy flow rate of state 12 may be found as:

$$\dot{H}_{12} = \dot{H}_{11} + \sum_{l=1}^{2}\left(\dot{n}_{8,l}\cdot\overline{h}_{8,l}\right) - \sum_{l=1}^{2}\left(\dot{n}_{9,l}\cdot\overline{h}_{9,l}\right) \quad (19)$$

From an energy balance around the control volume enclosing the dryer, enthalpy flow rate of state 13b may be found as

$$\dot{H}_{13b} = \sum_{m=1}^{4}\left(\dot{n}_{11,m}\cdot\overline{h}_{14,m}\right) + \dot{n}_{C_xH_yO_z}\cdot\left(\overline{h}_{2,C_xH_yO_z} + m_2\cdot\overline{h}_{2,H_2O(l)} + (m_1 - m_2)\cdot\overline{h}_{2,H_2O(v)} - \overline{h}_{1,C_xH_yO_z} - m_1\cdot\overline{h}_{1,H_2O(l)}\right) \quad (20)$$

where m denotes CO_2, H_2O, O_2 and N_2.

The specific enthalpy for state 16 may be written as

$$\overline{h}_{16} = \overline{h}_{15} + \frac{\nu_{15}\cdot(P_{16} - P_{15})\cdot M_{H_2O}}{\eta_{pump}} \quad (21)$$

At this point, we can calculate the total heat added to the gasifier as:

$$\dot{Q}_{added} = q_{added}\cdot\dot{n}_{C_xH_yO_z} \quad (22)$$

Enthalpy flow rate of state 13a can be calculated as

$$\dot{H}_{13a} = \dot{H}_{13b} + \dot{Q}_{added} \quad (23)$$

From an energy balance around the control volume enclosing the steam generator, the molar flow rate of steam generated may be found as

$$\dot{n}_{17} = \frac{\dot{H}_{12} - \dot{H}_{13a}}{\overline{h}_{17} - \overline{h}_{16}} \quad (24)$$

Work input to pump may be given as

$$\dot{W}_{pump} = \dot{n}_{17}\cdot\left(\overline{h}_{16} - \overline{h}_{15}\right) \quad (25)$$

Change of enthalpy flow rate of the process may be shown as

$$\Delta\dot{H}_{process} = \left(\dot{n}_{17} - \dot{n}_{C_xH_yO_z}\cdot\lambda\right)\cdot\left(\overline{h}_{18} - \overline{h}_{15}\right) \quad (26)$$

Net electrical power output of the system may be given as

$$\dot{W}_{net} = n_{stack}\cdot n_{cps}\cdot w_{SOFC}\cdot\eta_{inv} - \dot{W}_{blower} - \dot{W}_{pump} \quad (27)$$

Electrical efficiency, fuel utilization efficiency, and power-to-heat ratio may be calculated using Eqs. (28)–(30), respectively.

$$\eta_{el} = \frac{\dot{W}_{net}}{\dot{n}_{C_xH_yOz}\cdot\left(LHV + m_1\cdot\overline{h}_{fg}\right)} \quad (28)$$

$$FUE = \frac{\dot{W}_{net} + \Delta\dot{H}_{process}}{\dot{n}_{C_xH_yO_z}\cdot\left(LHV + m_1\cdot\overline{h}_{fg}\right)} \quad (29)$$

$$PHR = \frac{\dot{W}_{net}}{\Delta\dot{H}_{process}} \quad (30)$$

After energy analysis is completed, exergy analysis is conducted. In this analysis, exergy balance which is derived by combining first and second laws of thermodynamics [13] is applied to the control volumes enclosing the components. The steady state form of control volume exergy balance may be given as

$$0 = \sum_j\left(1 - \frac{T_o}{T_j}\right)\cdot\dot{Q}_j - \dot{W}_{cv} + \sum_i \dot{n}_i\cdot ex_i - \sum_e \dot{n}_e\cdot ex_e - \dot{E}x_D \quad (31)$$

In Eq. (31), ex represents the specific molar exergy. The components of specific exergy are discussed below. $\dot{E}x_D$ represents the exergy destruction in the control volume. Exergy losses are included in the fourth term of Eq. (31).

If we neglect the magnetic, electrical, nuclear, kinetic and potential effects, there are mainly two types of exergy: pyhsical and chemical. The first one measures the amount of work when the system comes into thermal ($T = T_o$) and mechanical ($P = P_o$) equilibrium. This condition is called as restricted dead state. Chemical exergy gives the amount of work when the system is brought from restricted dead state to dead state. At dead state, in addition to the thermal and mechanical equilibrium, the system is also at chemical equilibrium ($\mu = \mu_o$).

The physical flow exergy for simple, compressible pure substances is given as:

$$ex^{PH} = (h - h_o) - T_o(s - s_o) \quad (32)$$

Chemical exergy may be found using the tables available in the literature [14]. For an ideal gas mixture, Eq. (33) can be used to calculate the specific molar chemical exergy of the mixture.

$$ex^{CH} = \sum x_k \cdot e\bar{x}_k^{CH} + \bar{R} \cdot T_o \cdot \sum x_k \cdot \ln x_k \quad (33)$$

The exergy destruction rate in a component may be compared to the exergy rate of the fuel provided to the overall system using the exergy destruction ratio, as follows:

$$y_D = \frac{\dot{E}x_D}{\dot{E}x_F} \quad (34)$$

The exergy destruction rate of a component may be compared to the total exergy destruction rate within the system using the following equation:

$$y_D^* = \frac{\dot{E}x_D}{\dot{E}x_{D,tot}} \quad (35)$$

The exergy loss ratio is used to compare the exergy loss rate to the exergy rate of the fuel provided to the overall system.

$$y_L = \frac{\dot{E}x_L}{\dot{E}x_F} \quad (36)$$

In defining the exergetic efficiency, it is necessary to identify both a product and a fuel for the thermodynamic system being analyzed. The product represents the desired output produced by the system. The fuel represents the resources expended to generate the product. Exergetic efficiency of a component or system may be given as

$$\varepsilon = \frac{\dot{E}_P}{\dot{E}_F} = 1 - \frac{\dot{E}_D + \dot{E}_L}{\dot{E}_F} \quad (37)$$

Exergetic efficiency of the system can also be defined in terms of exergy destruction ratio and exergy loss ratio.

$$\varepsilon = 1 - \sum y_D - \sum y_L \quad (38)$$

For the integrated system studied in this paper, exergetic efficiency of the system may be defined as:

$$\varepsilon = \frac{\dot{W}_{net} + \Delta\dot{E}x_{process}}{\dot{E}x_{ch,C_xH_yO_z} + \dot{n}_{15} \cdot \bar{e}_{ch,H_2O(l)}} \quad (39)$$

$\dot{E}x_{ch,C_xH_yO_z}$ can be found using the correlation given by Szargut [14]. The correlation is modified for this study as follows:

$$\dot{E}x_{ch,C_xH_yO_z} = \beta \cdot \left[\dot{n}_{C_xH_yO_z} \cdot (LHV + m_1 \cdot \bar{h}_{fg})\right] \quad (40)$$

where β is defined for solid C,H,O,N compounds (for $O/C < 2$) as [14]

$$\beta = \frac{1.044 + 0.016 \cdot H/C - 0.3493 \cdot O/C \cdot (1 + 0.0531 \cdot H/C) + 0.0493 \cdot N/C}{1 - 0.4124 \cdot O/C} \quad (41)$$

Change of exergetic rate of process may be given as

$$\Delta\dot{E}x_{process} = (\dot{n}_{17} - \dot{n}_{C_xH_yO_z} \cdot \lambda) \cdot (ex_{18} - ex_{15}) \quad (42)$$

More information on exergy and its applications can be found in [15].

4. Results and discussion

The input data used in this study are shown in Table 1. Using this data, syngas composition is first calculated and shown in Table 2. As it can be seen from this table, when enriched oxygen is used instead of air, molar ratio of all species except nitrogen increases due to sending less amount of nitrogen to the gasifier. In the case of using steam as gasification agent, the molar ratios of gases that are used as fuel in SOFC, i.e. CH_4,

Table 1 – Input data.

Environmental temperature	25 °C
Fuel	
Type of biomass	Wood
Ultimate analysis of biomass [%wt dry basis]	50% C, 6% H, 44% O
Moisture content in biomass [%wt]	40%
Gasifier	
Moisture content in biomass entering gasifier [%wt]	20%
Temperature of syngas exiting gasifier	900 °C
Molar ratio of steam entering to gasifier to dry biomass	0.1
Molar composition of enriched oxygen	35% O_2, 65% N_2
SOFC	
Power requirement of SOFC	10 kW
Number of cells per stack	50
Temperature of syngas entering SOFC	850 °C
Temperature of air entering SOFC	850 °C
Pressure of the cell	1 atm
Cell voltage	0.65
Excess air coefficient	7
Active cell area	10×10 cm^2
Number of repeat elements per single cell	18
Flow configuration	Co-flow
Manufacturing type	Electrolyte-supported
Thickness of air channel	0.1 cm
Thickness of fuel channel	0.1 cm
Thickness of interconnect	0.3 cm
Thickness of anode	0.005 cm
Thickness of electrolyte	0.015 cm
Thickness of cathode	0.005 cm
Emissivity of PEN	0.8
Emissivity of interconnect	0.1
Diffusivity of anode	0.91 cm^2/s
Diffusivity of cathode	0.22 cm^2/s
Porosity of anode	0.5
Porosity of cathode	0.5
Turtuosity of anode	4
Turtuosity of cathode	4
Balance of plant	
Temperature of exhaust gas leaving the system	127 °C
Pressure ratio of blowers	1.18
Isentropic efficiency of blowers	0.53
Pressure ratio of pump	1.2
Isentropic efficiency of pump	0.8
Inverter efficiency	0.95

Table 2 – Syngas composition (molar basis).

	x_{CH_4}	x_{H_2}	x_{CO}	x_{CO_2}	x_{H_2O}	x_{N_2}
Case1: Air	0.14%	11.22%	8.16%	12.95%	22.68%	44.84%
Case2: Enriched O_2	0.28%	15.74%	11.40%	16.37%	28.80%	27.41%
Case3: Steam	2.15%	43.37%	27.38%	8.98%	18.12%	0.00%

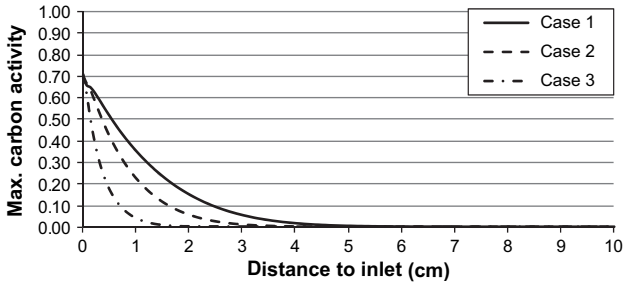

Fig. 2 – Change of maximum carbon activity with distance.

H_2 and CO, are higher than the cases when we use air or enriched oxygen; however the molar ratio of H_2O is lower than the other cases according to chemical equilibrium calculations.

After finding the syngas composition, heat transfer model of the SOFC is used to find the fuel cell related output parameters. First, recirculation ratio is taken as zero and the code is run until a fuel utilization of 0.85 is obtained. At this point, the maximum carbon activity through the channel length is checked. If this value is less than 1 for all the nodes, then there is no carbon deposition problem. If this value is higher than 1 for any nodes, then the calculations should be repeated with higher recirculation ratios until the carbon deposition is prevented. Fig. 2 shows that maximum carbon activity is less than 1 for all the nodes for all cases even if we do not recirculate the depleted fuel.

Fig. 3 shows the current density distribution for each case. Since the molar ratio of gas species used as fuel in SOFCs, e.g. CH_4, H_2 and CO, is higher for case-3, higher current densities for each node are obtained for this case compared to other cases. From Table 3, it can be seen that average current densities for cases 1, 2, and 3 are 0.240, 0.246, and 0.343 A/cm^2, respectively. It can also be followed from this table that power density for case-3 is higher than the other cases because we consider the cell voltage as constant in the modeling and average current density is higher for case-3 than other cases. It is also found that 13 stacks are needed for cases 1 and 2, whereas only 9 stacks are needed for case-3. This result shows that the purchase equipment cost for case-3 is lower than the other cases.

2-D temperature distributions of SOFCs are given in Figs. 4–6. From these figures, it is seen that temperature gradient in the flow direction is the highest in case-3. Case-2 and case-1 follow it, respectively. It should be noted that the temperature

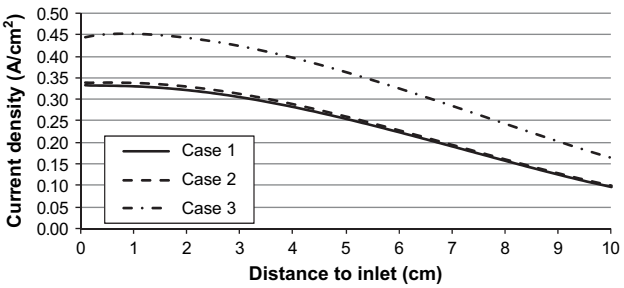

Fig. 3 – Change of current density with distance.

Table 3 – Recirculation ratio, Reynolds Number, average current density, fuel utilization ratio, number of stacks.

	r	Re	$i_{c,ave}$ [A/cm^2]	U_F	W_{sofc} [W/cm^2]	n_{stack}
Case1: Air	0	10.0	0.240	0.85	0.156	13
Case2: Enriched O_2	0	6.5	0.246	0.85	0.160	13
Case3: Steam	0	1.5	0.343	0.85	0.223	9

gradients are still less than the maximum allowable value that could cause thermomechanical instability.

Mass flow rates of substances entering the system are given in Table 4. It can be seen in this table that, for case-1, we need to feed more biomass to the system, which increases the cost of fuel. In addition, wood needs to be cut into small pieces before feeding to the system, hence equipment and operation cost for pretreatment of wood increases for this case. The energy input for the pretreatment operation of wood also increases. However, it should be noted that pretreatment of wood except drying is not taken into account in the analyses. From Table 4, the mass flow rate of air and water fed to the system, and steam produced and sent to the users can be seen. For case-3, fewer amounts of air and water are fed to the system, which in turn decreases the costs associated with the operation of blowers and pump. However, less amount of steam is produced for this case due to sending high amount of steam to the gasifier for initiating the gasification reactions.

Power input to the auxiliary components and power output from the system are shown in Table 5. It can be followed from this table that net power output for case-2 is the highest, which is mainly due to higher amount of power obtained for the given number of stacks. Change of enthalpy rate of the process is found to be the highest for case-1 and lowest for case-3. This is because allothermal gasification is used in case-3 and considerable amount of energy is spent in the gasification process, hence less energy remains for producing steam.

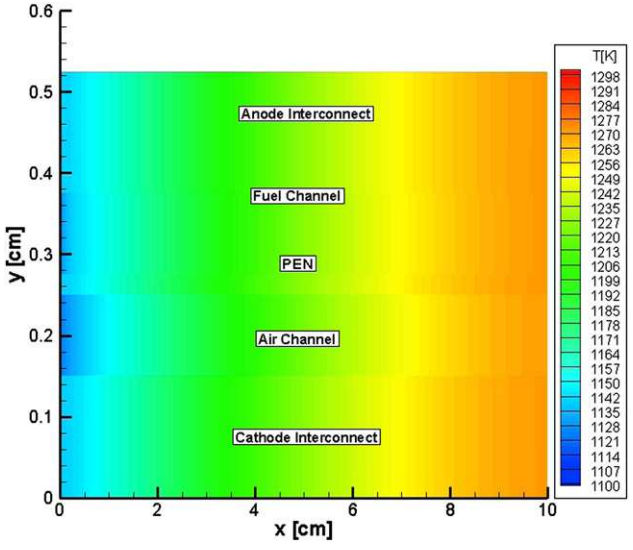

Fig. 4 – 2-D temperature distribution of SOFC for case-1 (Air gasification).

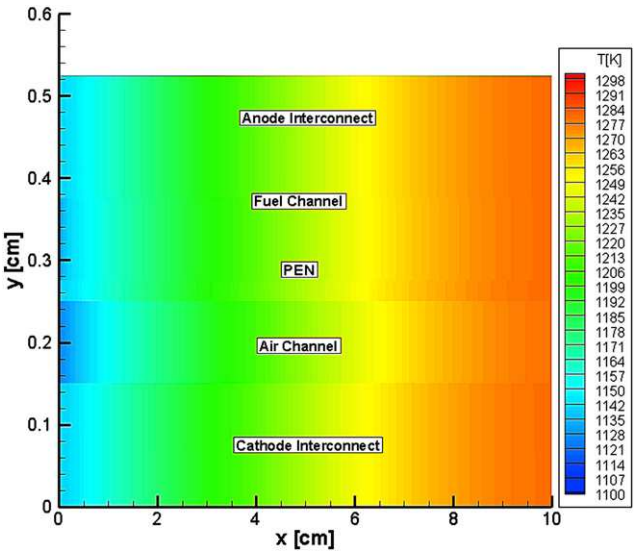

Fig. 5 – 2-D temperature distribution of SOFC for case-2 (Enriched oxygen gasification).

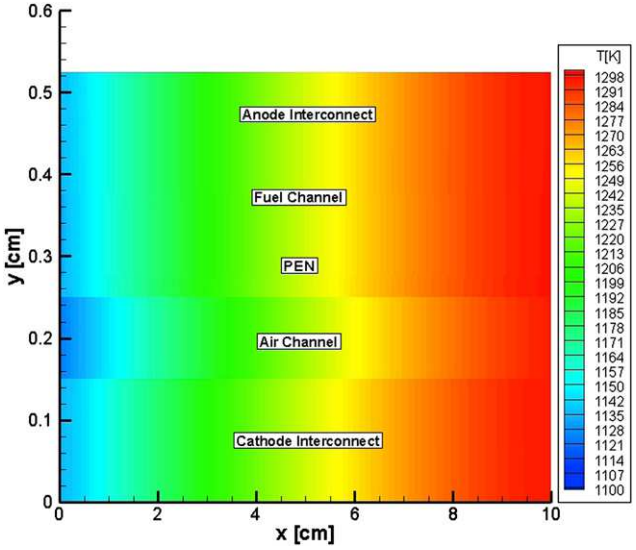

Fig. 6 – 2-D temperature distribution of SOFC for case-3 (Steam gasification).

Electrical efficiency, fuel utilization efficiency, power-to-heat ratio, and exergetic efficiency are chosen as performance assessment parameters in this study. The values of these parameters are shown in Table 6. It can be seen from this table that case-3 has the highest electrical efficiency. However, it has also the lowest fuel utilization efficiency since considerable amount of steam is sent to the gasifier and less steam is sent for process heating purposes. In general, producing electricity is more expensive than producing heat. If we compare the power-to-heat ratios, we can see that case-3 is the highest. It may be interpreted from this result that the primary purpose of using the system in case-3 should be producing electricity rather than producing heat. Exergetic efficiency is another way of comparing the overall system performance. In this comparison, the quality of the energy forms together with the quantity of the energy forms is considered. It is seen from Table 6 that exergetic efficiency for case-3 is the highest. When we combine all the results for performance assessment parameters, we can conclude that steam should be selected as the gasification agent to have a better performance of the system.

Table 4 – Mass flow rate of substances entering the system.

	$\dot{m}_{biomass}$ [g/s]	$\dot{m}_{air}$ (B1) [g/s]	$\dot{m}_{air}$ (B2) [g/s]	$\dot{m}_{water}$ [g/s]	$\dot{m}_{steam}$ [g/s]
Case1: Air	4.048	7.796	45.648	7.654	7.654
Case2: Enriched O_2	3.867	6.989	46.841	6.604	6.604
Case3: Steam	1.826	–	45.219	0.767	0.685

We can also use air and steam or enriched oxygen and steam gasification agents in the integrated SOFC and biomass gasification systems. In these systems, molar ratio of oxidant to dry biomass and molar ratio of steam to dry biomass may be altered to get different results. However, we expect that such output parameters will be between those obtained from only when one of the gasification agents is used. For example, if we choose enriched oxygen and steam gasification case, it is expected that the electrical efficiency will be between 19.9% and 41.8% and fuel utilization efficiency will be between 50.8% and 60.9%, based on the efficiencies shown in Table 6.

Exergy destructions in the components and exergy destruction ratios are calculated and the results are shown in Tables 7 and 8. The results show that, for cases 1 and 2, the largest portion of exergy is destructed in the gasifier. This destruction accounts for 31.02% for case-1 and 30.89% for case-2 of the exergy of the fuel, and 48.60% for case-1 and 48.15% for case-2 of the total exergy destructions. For case-3, the magnitude of exergy destruction for gasifier is much lower than that for cases 1 and 2 because of using allothermal gasification for this case. In this case, the highest exergy is destructed in the heat exchanger, which is 25.65% of the exergy of the fuel and 46.44% of the total exergy destructions. Exergy losses to the environment are also calculated. The exergy losses are found as 2676 W, 2489 W, and 1281 W for cases 1, 2, and 3, respectively. When we compare the exergy loss ratios, it is seen that case-3 has

Table 5 – Power demand for auxiliary components, net power and heat output.

	$\dot{W}_{SOFC}$ [W]	$\dot{W}_{blower-1}$ [W]	$\dot{W}_{blower-2}$ [W]	$\dot{W}_{pump}$ [W]	$\dot{W}_{net}$ [W]	$\Delta\dot{H}_{process}$ [W]
Case1: Air	10140	227.5	1332.1	0.2	8073.2	19741.3
Case2: Enriched O_2	10384	204.0	1366.9	0.2	8293.7	17032.9
Case3: Steam	10031	–	1319.6	0.02	8210.2	1765.9

Table 6 – Performance assessment parameters.

	η_{el}	FUE	PHR	ε
Case1: Air	18.5%	63.9%	0.409	30.9%
Case2: Enriched O_2	19.9%	60.9%	0.487	30.7%
Case3: Steam	41.8%	50.8%	4.649	39.1%

Table 7 – Exergy destructions in the components.

Component	Exergy destruction [W]		
	Case 1	Case 2	Case 3
SOFC	664	692	845
Gasifier	15727	14952	837
Afterburner	1622	1800	1490
Dryer	3018	2884	1336
Gas cleanup	678	507	164
Heat exchanger	6421	6453	5834
Blower-1	217	195	–
Blower-2	1272	1305	1260
ASU	–	4	–
Steam generator	2235	1740	295
Water pump	0	0	0
Inverter	507	519	502

Table 8 – Exergy destruction ratios.

	Case 1		Case 2		Case 3	
	y_D [%]	y_D^*[%]	y_D [%]	y_D^* [%]	y_D [%]	y_D^* [%]
SOFC	1.31	2.05	1.43	2.23	3.71	6.72
Gasifier	31.02	48.60	30.89	48.15	3.67	6.67
Afterburner	3.20	5.01	3.72	5.80	6.55	11.86
Dryer	5.95	9.33	5.96	9.29	5.88	10.64
Gas cleanup	1.34	2.09	1.05	1.63	0.72	1.30
Heat exchanger	12.66	19.84	13.33	20.78	25.65	46.44
Blower-1	0.43	0.67	0.40	0.63	0.00	0.00
Blower-2	2.51	3.93	2.70	4.20	5.54	10.03
ASU	–	–	0.00	0.01	0.00	0.00
Steam generator	4.41	6.91	3.59	5.61	1.30	2.35
Water pump	0.00	0.00	0.00	0.00	0.00	0.00
Inverter	1.00	1.57	1.07	1.67	2.21	3.99

the highest exergy loss ratio, which is equal to the 5.63% of the exergy of the fuel. Case-1 (5.28%) and case-2 (5.14%) follow it, respectively.

5. Conclusions

An analysis for integrated SOFC and biomass gasification systems is developed. For this purpose, a heat transfer model for the SOFC part and thermodynamic models for the rest of the components are used. The effect of gasification agent on the performance of the system is discussed. This study shows that using steam as the gasification agent yields the highest electrical efficiency, power-to-heat ratio and exergetic efficiency, but the lowest fuel utilization efficiency. It is also found that the largest portion of exergy is destructed at the gasifier for air and enriched oxygen gasification cases and the heat exchanger used for heating the air entering the SOFC for steam gasification case.

Acknowledgment

The financial and technical support of an Ontario Premier's Research Excellence Award, the Natural Sciences and Engineering Research Council of Canada, EcoEnergy Technology Initiative Program, AAFC-NRC Bioproducts Program, Carleton University and University of Ontario and Institute of Technology is gratefully acknowledged.

Nomenclature

C	weight percentage of carbon in biomass
ex	specific molar exergy, J/mole
$\dot{E}x$	exergy flow rate, W
FUE	fuel utilization ratio
$\overline{h}$	specific molar enthalpy, J/mole
H	weight percentage of hydrogen in biomass
$\dot{H}$	enthalpy flow rate, W
K	chemical equilibrium constant
LHV	lower heating value, J/mole
m	molar ratio of water to dry biomass
M	molecular weight, g/mole
n	number
$\dot{n}$	molar flow rate, mole/s
N	weight percentage of nitrogen in biomass
O	weight percentage of oxygen in biomass
P	pressure, bar
PHR	power-to-heat ratio
q	specific molar heat, J/mole
$\dot{Q}$	heat rate, W
R	universal gas constant, J/mole-K
T	temperature, K
y	exergetic ratio
w	power output of a single cell, W
$\dot{W}$	power output, W
x	molar concentration

Greek letters

ρ	density, g/cm^3
η	efficiency
$\Delta\overline{g}$	change in specific molar gibbs free energy, J/mole
υ	specific volume, cm^3/g
ε	exergetic efficiency
β	exergetic correlation constant
λ	molar ratio of steam entering the gasifier to the dry biomass
μ	chemical potential, J/mole

Subscripts

cps	cell per stack
CV	control volume
D	destruction

el	electrical
inv	inverter
F	fuel
fc	fuel cell
fg	difference in property for saturated vapor and saturated liquid
L	loss
m	methanation
o	standard
P	product
req	required
tot	total
wgs	water gas shift reaction

Superscripts

CH	chemical
PH	physical

REFERENCES

[1] Goldemberg J, Johansson TB, editors. World energy assessment: overview 2004 update. New York, U.S.A: United Nations Development Programme; 2004.

[2] Renewables in global energy supply. An IEA fact sheet. France: International Energy Agency; 2007.

[3] Xenergy. 2002. Toward a renewable power supply: the use of bio-based fuels in stationary fuel cells.

[4] Schmersahl R, Scholz V. Testing a PEM fuel cell system with biogas fuel. Agricultural Engineering International: the CIGR Ejournal 2005;7. Manuscript EE 05 002.

[5] Panopoulos KD, Fryda LE, Karl J, Poulou S, Kakaras E. High temperature solid oxide fuel cell integrated with novel allothermal biomass gasification part I: modelling and feasibility study. Journal of Power Sources 2006a; 159:570–85.

[6] Panopoulos KD, Fryda LE, Karl J, Poulou S, Kakaras E. High temperature solid oxide fuel cell integrated with novel allothermal biomass gasification part II: exergy analysis. Journal of Power Sources 2006b;159:586–94.

[7] Cordiner S, Feola M, Mulone V, Romanelli F. Analysis of a SOFC energy generation system fuelled with biomass reformate. Applied Thermal Engineering 2007;27:738–47.

[8] Athanasiou C, Coutelieris F, Vakouftsi E, Skoulou V, Antonakou E, Marnellos G, et al. From biomass to electricity through integrated gasification/SOFC system-optimization and energy balance. International Journal of Hydrogen Energy 2007;32:337–42.

[9] Omosun AO, Bauen A, Brandon NP, Adjiman CS, Hart D. Modelling system efficiencies and costs of two biomass-fuelled SOFC systems. Journal of Power Sources 2004;131:96–106.

[10] Colpan CO. 2009. Thermal modeling of solid oxide fuel cell based biomass gasification systems. PhD thesis. Department of Mechanical and Aerospace Engineering, Carleton University.

[11] Colpan CO, Dincer I, Hamdullahpur F. Thermodynamic modeling of direct internal reforming solid oxide fuel cells operating with syngas. International Journal of Hydrogen Energy 2007;32:787–95.

[12] Achenbach E. 1996. SOFC Stack Modelling. Final Report of Activity A2, Annex II: Modelling and Evaluation of Advanced Solid Oxide Fuel Cells, International Energy Agency Programme on R, D&D on Advanced Fuel Cells, Juelich, Germany.

[13] Bejan A, Tsatsaronis G, Moran M. Thermal design and optimization. U.S.A: John Wiley and Sons Inc; 1996.

[14] Szargut J. Exergy method-technical and ecological applications. Boston: WIT Press; 2005.

[15] Dincer I, Rosen MA. Exergy: energy, environment and sustainable development. UK: Elsevier; 2007.